

Applications of Lasers to Collision Studies*

W. R. MacGillivray and M. C. Standage

Division of Science and Technology, Griffith University,
Nathan, Qld 4111, Australia.

Abstract

A review is presented of theoretical and experimental aspects of the application of lasers to the field of electron-atom collision physics. Experimental techniques are briefly reviewed and various theoretical treatments of the laser-atom interaction are dealt with in some detail.

1. Introduction

The introduction of lasers to the study of collision processes followed the development of tunable dye lasers in the early 1970s. Laser techniques have now been applied to the investigation of superelastic scattering, stepwise excitation, photon recoil, spin-polarised collisions, Rydberg atom collisions and laser-assisted collisions. All these techniques depend upon one or more of the characteristic properties of laser light, its very high intensity, spectral resolution and polarisation.

An understanding of the interactions between laser light and matter is clearly an essential aspect of the successful application of lasers to the investigation of collision processes. Theoretical methods for treating such interactions include perturbation theory, which is appropriate for weak optical excitation; rate equations and more sophisticated, non-perturbative treatments, such as semiclassical density matrix and Heisenberg operator techniques.

In this paper, a review is presented of experimental and theoretical techniques currently in use in which lasers are applied to the investigation of collision processes. Although the main purpose of this paper is to review such techniques as they apply to electron-atom collisions, some of the techniques discussed are either currently used to study other types of collision processes, such as ion-atom collisions, or could be.

2. Experimental Applications of Laser Techniques to Atomic Collision Studies

(a) Stepwise Excitation and Superelastic Scattering

Fig. 1 shows two types of stepwise excitation schemes and a superelastic scattering scheme. In scheme I, electron excitation from the ground state $|g\rangle$

* Paper presented at the Workshop on Interfaces in Molecular, Electron and Surface Physics, held at Fremantle, Australia, 4-7 February 1990.

to the first excited state $|e\rangle$ is followed by laser excitation to the higher excited state $|i\rangle$. The intensity and polarisation of the light emitted as the atom decays from state $|i\rangle$ to state $|f\rangle$ enables information about the initial electron excitation process from the ground state to be obtained. In scheme II, laser excitation from the ground state is followed by electron excitation between the excited states, with the fluorescence emission providing information on inelastic processes between excited states. The superelastic scattering process shown in Scheme III involves laser excitation from $|g\rangle$ to $|e\rangle$ followed by de-excitation due to electron impact.

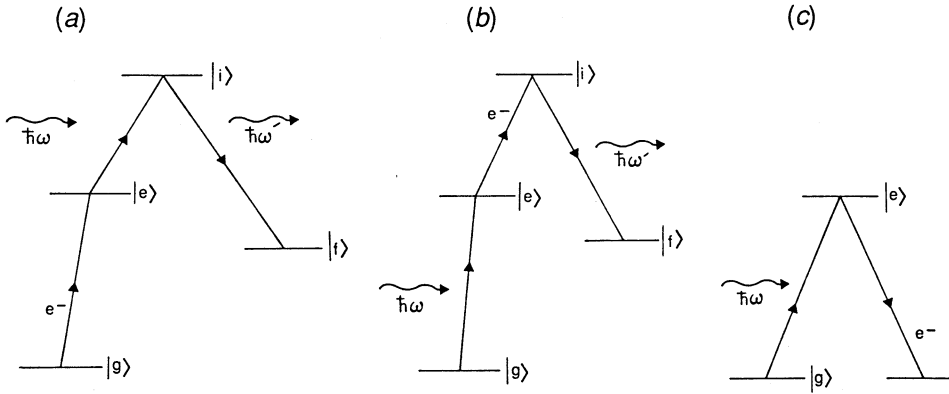


Fig. 1. (a) Electron–laser stepwise excitation scheme I. (b) Electron–laser excitation scheme II. (c) Superelastic scattering excitation scheme III.

Since the early 1970s, considerable interest has been focussed on the development of experimental methods that enable scattering processes to be completely characterised. Such experiments were first realised with the development of two techniques, the electron–photon coincidence technique of Eminyán *et al.* (1974) and the superelastic scattering technique of Hertel and Stoll (1974, 1977). The electron–photon coincidence technique has recently been applied to a type I stepwise excitation scheme in the first demonstration of a stepwise electron–photon coincidence experiment (MacGillivray and Standage 1988; Murray *et al.* 1989).

The electron scattering processes can be represented by the electron scattering density operator ρ^e , which is given by the following expression (Blum 1981):

$$\rho_{mn}^e = \frac{1}{2J_g + 1} \sum_{m_g m_i m_f} \langle J m m_f | T | J_g m_g m_i \rangle \langle J_g m_g m_i | T^\dagger | J n m_f \rangle, \quad (1)$$

where T is the electron excitation operator, $|J_g m_g m_i\rangle$ and $|J n m_f\rangle$ are substates of the initial and final states respectively, and m_i and m_f are the incident and scattered electron spin projection quantum numbers. Matrix elements of ρ^e possess several symmetry properties that reflect the Hermitian nature of the operator and depend upon the axial or planar symmetry character of the scattering processes being considered.

In the case of planar symmetry scattering processes, such as occur in superelastic and electron-photon correlation studies (for a comparison of superelastic and electron-photon correlation techniques see Farrell *et al.* 1989; MacGillivray and Standage 1990) in which a scattering plane is defined by the incident and scattered electrons, the off-diagonal density matrix elements of the electron scattering density operator are in general nonzero.

The superelastic scattering technique uses laser excitation of atoms in an atomic beam which are optically pumped by the laser into an aligned or oriented excited state. These atoms are de-excited by a beam of electrons directed into the interaction region and superelastically scattered electrons produced in the scattering process are detected by an electron analyser. The atomic collision parameters are obtained by measuring the superelastic differential cross section as a function of the laser beam polarisation.

By appealing to the principle of microreversibility, it can be shown that the electron scattering processes for a superelastic process can be represented by the complex conjugate of the usual electron scattering density operator ρ^e used to represent electron excitation processes.

In a superelastic experiment, the experimental parameter measured is the differential cross section σ of the superelastically scattered electrons that have gained energy in de-exciting the target atoms. The theoretical form of this signal is given by (MacGillivray and Standage 1988, 1990);

$$\sigma = \sum_{mn} O_{mn}^e \rho_{nm}^{e*}, \quad (2)$$

where O_{mn}^e are density matrix elements that represent the excited state populations and coherences formed in the optical pumping process.

Experimental geometries employed in superelastic scattering experiments have placed the laser beam parallel to the scattering plane, perpendicular to it, or at some intermediate angle. The in-plane geometry enables the magnitude of diagonal and off-diagonal electron scattering density operator matrix elements to be obtained by measuring superelastic differential cross sections with the laser beam polarised parallel and then perpendicular to the scattering plane. The out-of-plane geometries enable a full determination of the magnitudes and signs of the matrix elements to be made, including a measurement of the coherence of the collisional process.

The initial experiments of Hertel and Stoll (1974) were performed on e^- -Na atom collisions, over the energy range 5.1 eV to 22.1 eV and with the laser beam incident in the scattering plane. Later measurements by this group (Hermann *et al.* 1980) were performed with the laser beam incident from out of the plane. Other superelastic scattering experiments on sodium have been performed by Scholten *et al.* (1988) and Farrell *et al.* (1989) using a laser beam perpendicular to the scattering plane. For this geometry, a determination of the laser induced line polarisation is also required to analyse the data.

Spin polarisation studies have been reported by two groups. Hanne *et al.* (1982) used a Mott detector to apply spin analysis to an unpolarised beam of electrons superelastically scattered from Na at 20 eV. Their measured spin polarisations were 0.095 ± 0.048 and -0.068 ± 0.044 respectively for scattering

off the $3^2P_{1/2}$ and $3^2P_{3/2}$ excited states of Na. McClelland *et al.* (1989; see other references therein) have performed a series of experiments in which a spin polarised beam of electrons was superelastically scattered off laser excited $3^2P_{3/2}$ sodium atoms. The polarised electrons were produced by a GaAs photocathode excited by a diode laser. The laser beam was incident at right angles to the scattering plane and was either circularly or linearly polarised. Superelastic scattering measurements were performed with the spin of the incident electron beam either up or down with respect to the scattering plane. The spin asymmetry was measured as a function of electron scattering angle using linearly polarised light. The use of circularly polarised light allowed the resolution of singlet and triplet contributions to the angular momentum transferred between the electron and the atom in the collision process and gave a measurement of the ratio of triplet to singlet differential cross sections.

A superelastic scattering experiment has been performed by Register *et al.* (1978, 1983) on barium using a single mode laser to isolate the $I = 0$ nuclear spin isotopes. The laser beam was incident in the scattering plane. An unexpected asymmetry in the superelastic scattering signal was observed at small electron scattering angles. It has recently been established by Zetner *et al.* (1989) that the cause of this anomaly is due to the finite volume of the interaction region and detector solid angles.

Stepwise excitation techniques have been recently reviewed by MacGillivray and Standage (1988). In this paper, an overview is presented and readers are referred to the above reference for a more detailed account.

In type I stepwise excitation experiments, the intensity and polarisation of photons are detected in the spontaneous emission process from state $|i\rangle$ to $|f\rangle$. The fluorescent intensity is given by

$$I = \sum_{m'n',mn} F_{n'm'} A_{m'n'mn} \rho_{mn}^e. \quad (3)$$

The terms $A_{m'n'mn}$ represent either decay constants or Rabi frequencies associated with the laser excited transition. Matrix elements of the fluorescence emission operator F are given by

$$F_{n'm'} = \sum_q \langle n' | \mathbf{f} \cdot \mathbf{P} | q \rangle \langle q | \mathbf{f}^* \cdot \mathbf{P} | m' \rangle, \quad (4)$$

where \mathbf{f} is the polarisation vector of the optical analyser, \mathbf{P} is the electric dipole moment operator and $|q\rangle$ are substates of the final state $|f\rangle$.

For type II stepwise excitation schemes, it can be shown that the fluorescent intensity is given by

$$I = \sum_{m'n',mn} F_{n'm'} O_{mn}^e f_{m'm} f_{n'm}^*, \quad (5)$$

where O_{mn}^e are matrix elements of the optical excitation operator for the laser excited step and $f_{m'm}$ are amplitudes representing electron excitation between substates of the the excited states $|e\rangle$ and $|i\rangle$.

Type I excitation schemes have been used to investigate electron collisions with neon, calcium, mercury and helium atoms. An important aspect of some of these investigations is the use of the stepwise technique to study the impact excitation of metastable atoms. Absolute cross section measurements have been made using stepwise excitation techniques on the $2p^5(3s)$ states of neon, including the metastable states $1s_5(^3P_2)$ and $1s_3(^3P_0)$ as well as the states $1s_2(^1P_1)$ and $1s_4(^3P_1)$ (for details see Phillips *et al.* 1981*a*, 1981*b*; Miers *et al.* 1982; Phelps *et al.* 1982; Zetner *et al.* 1986). The calcium investigations were performed by Dobryshin *et al.* (1982) and produced absolute total cross sections for the $4^3P_{0,1,2}$ states. Zetner *et al.* (1986) also investigated the cross section of the helium 2^1S metastable state near threshold.

Type I experiments performed on e^- -Hg atom collisions have been used by McLucas *et al.* (1982*a*, 1982*b*) to investigate the role of spectroscopic structure in collision processes. The spectral resolution offered by a combination of single mode laser excitation and atomic beam techniques enables the hyperfine structure of the laser excited transition used in the stepwise excitation scheme to be resolved. Evidence was found that the Percival-Seaton hypothesis—that the nuclear spin plays no active part during the collision process—broke down near threshold for excitation of the 6^1P_1 state of mercury. It was suggested that a negative-ion resonance might be responsible for this effect. Relative total and partial cross section measurements were also obtained for the 6^1P_1 state.

The investigation of the electron impact excitation of the 6^3P_2 metastable state of mercury near threshold has been performed by two groups using c.w. single mode (Webb *et al.* 1985*b*) and pulsed laser (Hanne *et al.* 1985) techniques. It should be noted that in such experiments, the stepwise technique provides additional data, which are not otherwise available, on the partial total cross sections for the electron impact excitation of the metastable state. These data are accessible because two optical excitation/emission steps occur following the initial excitation of the $J = 2$ angular momentum state.

The extension of stepwise excitation techniques to electron-photon correlation studies has recently been reported by Murray *et al.* (1989) in an experiment which used mercury as the target species. This experimental technique combines the ability of the coincidence technique to completely characterise the electron excitation process with the advantages of the stepwise technique in being able to provide high spectral resolution and thereby directly eliminate the effects of spectroscopic structure in investigation of collisions, access VUV transitions and provide a new means of investigating the excitation of metastable states. Theoretical aspects of the stepwise correlation technique have been dealt with in Webb *et al.* (1984*a*, 1984*b*), MacGillivray and Standage (1988) and Murray *et al.* (1990*a*).

Type II stepwise excitation techniques that have so far been reported have involved the study of inelastically scattered electrons from laser excited sodium and barium atoms. Measurements were made by Hertel and Stoll (1974) of the differential cross sections for the 3^2P-4^2S and 3^2P-3^2D transitions, where the initial 3^2P state was prepared by laser excitation. Hermann *et al.* (1977) showed how angular correlation parameters could be obtained for these transitions using type II stepwise techniques. Their approach was similar to that used

for a superelastic scattering experiment except that inelastic differential cross sections are monitored as a function of laser polarisation.

Other experiments on the excited state total cross sections of the sodium 3P–3D transitions have been performed by Stumpf and Gallagher (1985). Differential cross sections for inelastic scattering off excited levels of barium have been performed by Register *et al.* (1978).

(b) Laser-assisted Collisions

In laser-assisted collisions, the laser photon can be thought of as having the role of a third body in a collision process which involves an atom, an electron and a photon. Initial experiments performed by Weingartshofer *et al.* (1977) were confined to elastic electron collisions in which the main interaction takes place between the free electron and the laser field. In effect, the electron gains or loses energy which corresponds to the absorption or emission of one or more laser photons in the presence of the atom. These are known as free-free or inverse Bremsstrahlung transitions with experiments being performed using both c.w. and pulsed CO₂ lasers and argon atoms.

Recently, Mason and Newell (1987, 1989) and Wallbank *et al.* (1988) have performed experiments in which the simultaneous electron and photon excitation of metastable states of atoms has been observed. It should be emphasised in these experiments, neither the electron or the photon by itself have sufficient energy to excite the transition. The process may be described by

$$e(E_i) + n\hbar\omega + A = A^* + e(E_i + n\hbar\omega - E_{\text{ex}}), \quad (6)$$

where E_i is the incident electron energy, E_{ex} is the excitation energy for the atomic transition and $\hbar\omega$ is the laser photon energy.

These experiments have so far been performed on the excitation of the metastable 2^3S state of helium with either a pulsed or c.w. CO₂ laser operating at $\hbar\omega = 0.117$ eV and with detection of the metastable atoms. It would seem possible to detect the scattered electrons and thereby obtain the differential cross section for such processes. The possibility of using other atoms, such as hydrogen with a Nd:YAG laser operating at $\hbar\omega = 1.17$ eV, has been discussed from a theoretical point of view by Francken and Attaourti (1988).

(c) Photon Recoil Techniques

Another application of lasers to atomic collision studies has been to use the photon recoil that results from the absorption of laser photons by the target atom, and the subsequent re-emission of spontaneously emitted photons, to physically deflect a highly collimated beam of atoms. In these experiments (see Jaduszliwer *et al.* 1984), the deflection produced by photon recoil and electron impact is used to determine ground and excited state cross sections. A variant of this type of experiment has been under development (Gallagher 1987) in which the Doppler shift of the target atoms is measured. Experiments reported in the literature which make use of photon recoil techniques have so far been confined to sodium.

3. The Theory of Laser-Atom Interactions

For the excitation of an atom with a weak optical field, it is assumed that only one photon is involved in the interaction and so the process can be treated as a weak perturbation. A typical weak excitation expression is (see e.g. MacGillivray and Standage 1988) for a stepwise type I excitation process:

$$\rho_{m'n'}^i = \frac{1}{\Gamma_i \Gamma_e} \sum_{mn} \langle m' | \mathbf{e} \cdot \mathbf{P} | m \rangle \langle m | \mathbf{e}^* \cdot \mathbf{P} | n' \rangle \rho_{mn}^e, \quad (7)$$

where Γ_i and Γ_e are the decay constants for the upper and lower states respectively, $\rho_{m'n'}^i$ and ρ_{mn}^e are the associated density matrix elements, \mathbf{e} is the laser polarisation and \mathbf{P} is the atomic dipole moment. The most important aspect of equation (7) is that it gives an analytical relationship between the density matrix elements of the states linked by the laser, which enables algebraic expressions for theoretical signals to be written. This greatly simplifies the theoretical analysis of the laser interaction with the atom and, as a consequence, weak excitation expressions should be used whenever possible.

However, there are many circumstances where the weak excitation approach is not applicable, such as occurs, for example, with optical pumping by lasers in superelastic scattering experiments. In such cases, other theoretical techniques must be considered and in the remainder of this paper three techniques are reviewed for treating the strong interaction of light with matter. The simplest of these techniques is the use of rate equations which make use of the Einstein A and B coefficients to describe the optical interactions. The limitation with rate equations is that they deal only with populations or, in terms of density matrix theory, diagonal density matrix elements and do not treat coherences, which are the off-diagonal density matrix elements.

Several techniques are available that do treat coherences and two methods are discussed below. These are the semiclassical density matrix technique, in which the radiative decay processes are included in an ad hoc manner in the density matrix equations, and the Heisenberg operator technique, which is a full quantum electrodynamical method in which the radiative decay processes form a natural part of the theory.

(a) Rate Equations and Semiclassical Density Matrix Equations

The interaction of a two-level quantum system with a monochromatic laser beam of optical frequency ω_L and energy density W provides a convenient case to compare rate equations and the semiclassical density matrix equations of motion. The two level system consists of a ground state $|g\rangle$ and an excited state $|e\rangle$ with an associated transition frequency ω_{eg} (Fig. 2a). The excited state is assumed to have a spontaneous emission decay rate of Γ and the absorption and stimulated emission decay rates are respectively B_{ge} and B_{eg} . In the case of a two-level system with no degeneracy, $B_{ge} = B_{eg} = B$.

As mentioned above, the rate equation method deals only with the populations of the energy levels and it can be readily shown that the appropriate rate

equations for a two-level system are

$$\begin{aligned}\dot{\rho}_{ee} &= -\Gamma\rho_{ee} + BW(\rho_{gg} - \rho_{ee}), \\ \dot{\rho}_{gg} &= \Gamma\rho_{ee} - BW(\rho_{ee} - \rho_{gg}),\end{aligned}\quad (8)$$

where the diagonal density matrix elements ρ_{ee} and ρ_{gg} represent the excited and ground state populations respectively.

In semiclassical density matrix theory (see e.g. Webb *et al.* 1984*b* for details), the time evolution of the quantum system is given by the equation of motion of the density matrix ρ ,

$$i\hbar\rho = [H, \rho] + \text{relaxation terms}, \quad (9)$$

where H consists of the sum of the free atom Hamiltonian and the interaction Hamiltonian. The relaxation terms have to be deduced from a knowledge of the relaxation mechanisms of the quantum system and inserted into equation (9). In the rotating wave approximation, the density matrix equations are given by

$$\dot{\rho}_{ee} = -\Gamma\rho_{ee} + \frac{1}{2}i\Omega(\rho_{eg} - \rho_{ge}), \quad (10a)$$

$$\dot{\rho}_{gg} = \Gamma\rho_{ee} - \frac{1}{2}i\Omega(\rho_{eg} - \rho_{ge}), \quad (10b)$$

$$\dot{\rho}_{eg} = -(i\Delta + \Gamma)\rho_{eg} + \frac{1}{2}i\Omega(\rho_{ee} - \rho_{gg}). \quad (10c)$$

The detuning of the laser from the Doppler shifted atomic transition frequency is given by

$$\Delta = \omega_L - \omega_{eg} - kV_z, \quad (11)$$

where Ω is the Rabi frequency given by

$$\Omega = -\mathbf{E} \cdot \mathbf{P}/\hbar. \quad (12)$$

The Rabi frequency is taken as real, where \mathbf{E} is the optical electric field of the laser and \mathbf{P} is atomic dipole operation. The appearance of the optical coherence terms ρ_{eg} and ρ_{ge} should be noted in equations (10).

The relationship between the rate equations (8) and the semiclassical density matrix equations (10) may be seen by applying the approximation that the rate of change of the optical coherence between the upper and lower states is zero, i.e. $\dot{\rho}_{eg} = 0$. This approximation applies either for the case that the interaction has occurred for a time sufficiently long that the state populations are nearly stationary, or the optical excitation is sufficiently weak that the populations do not ever change significantly. Equation (10c) then yields

$$\rho_{eg} = i\Omega(\rho_{ee} - \rho_{gg}) [2(i\Delta + \Gamma)]^{-1}. \quad (13)$$

Insertion of equation (13) and its complex conjugate into equations (10a) and (10b) gives

$$\begin{aligned}\dot{\rho}_{ee} &= -\Gamma\rho_{ee} + \Omega^2\Gamma[2(\Gamma^2 + \Delta^2)]^{-1}(\rho_{ee} - \rho_{gg}), \\ \dot{\rho}_{gg} &= \Gamma\rho_{ee} - \Omega^2\Gamma[2(\Gamma^2 + \Delta^2)]^{-1}(\rho_{ee} - \rho_{gg}).\end{aligned}\quad (14)$$

Comparison of equations (8) and (14) show that they are identical provided that

$$BW = \Omega^2\Gamma[2(\Gamma^2 + \Delta^2)]^{-1}.\quad (15)$$

If allowance is made for integrating over the laser line profile, then it can be shown that (Trajmar *et al.* 1990)

$$B\bar{W} = 2\pi\Omega^2,\quad (16)$$

where \bar{W} is the average laser power density per unit frequency of the laser beam.

(b) The Heisenberg Operator Method

When the laser excited atomic transition contains nearly degenerate energy levels due to spectroscopic effects such as fine or hyperfine structure, then for laser intensities at which power broadening becomes comparable with this spectroscopic structure, coherences can form between the sublevels that may play a significant role in the behaviour of the system and affect measured quantities such as the polarisation of the fluorescence emitted by the laser excited transition. To adequately describe this case requires the use of a full quantum electrodynamical theoretical treatment. Such a treatment was originally given by Ackerhalt *et al.* (1973) and Ackerhalt and Eberly (1974) for a two-state atom and extended to a three-state, stepwise excitation scheme by Whitley and Stroud (1976). Farrell *et al.* (1988), Murray *et al.* (1990) and Trajmar *et al.* (1990) have extended the treatment to an arbitrary number of states. This method makes use of the Heisenberg equations of motion for the atomic operator σ :

$$i\hbar\dot{\sigma} = [\sigma, H],\quad (17)$$

where H is the system Hamiltonian. The matrix elements of the atomic operator are formed by

$$\sigma_{ij} = |i\rangle\langle j|,\quad (18)$$

where $|i\rangle$ and $|j\rangle$ are states of the atomic system. The system evolves under the total Hamiltonian H , which is given by

$$H = H_A + H_F + H_I,\quad (19)$$

where H_A is the free atom Hamiltonian, H_F is the electromagnetic field Hamiltonian and H_I is the interaction Hamiltonian between the electromagnetic field and the atom.

The free atom Hamiltonian is written as

$$H_A = \sum_m E_m \sigma_{mm}, \quad (20)$$

where E_m is the energy of the substate $|m\rangle$. The field Hamiltonian is expressed in terms of photon annihilation and creation operators, such that

$$H_F = \hbar \sum_{\lambda} \omega_{\lambda} a_{\lambda}^{\dagger} a_{\lambda}, \quad (21)$$

where λ specifies both the polarisation and wave vector of the field modes. The interaction Hamiltonian is given by

$$H_I = \hbar \sum_e \sum_g \sum_{\lambda} (g_{eg}^{\lambda} \sigma_{eg} a_{\lambda} + g_{eg}^{\lambda*} a_{\lambda}^{\dagger} \sigma_{ge}), \quad (22)$$

where g_{eg}^{λ} is the coupling coefficient between a particular mode of the optical field and the atomic transition $|g\rangle - |e\rangle$. This Hamiltonian is said to be normally ordered, which Ackerhalt and Eberly (1974) have shown corresponds to a description of spontaneous emission in terms of the radiation reaction of the field upon the source.

The coupling coefficients for the dipole transitions are given by

$$g_{eg}^{\lambda} = -i \mathbf{e}_{\lambda} \cdot \mathbf{P}_{eg} (2\pi\omega_{\lambda}/\hbar V)^{\frac{1}{2}}, \quad (23)$$

where \mathbf{e}_{λ} is the polarisation vector of the λ mode of the radiation field, P_{eg} is the dipole operator matrix element $\langle e | \mathbf{P} | g \rangle$ and V is the interaction volume supporting the field modes.

The atomic operator elements relate to the density matrix elements by

$$\langle \sigma_{eg} \rangle = \langle \Psi | e \rangle \langle g | \Psi \rangle = \rho_{ge}, \quad (24)$$

where $|\Psi\rangle$ is a linear combination of the atomic states $|g\rangle$ and $|e\rangle$. The equations for the atomic operators are expressed in terms of slowly varying operators in the rotating frame using the transformation

$$\chi_{eg} = \sigma_{eg} e^{-i\omega_{\lambda} t}. \quad (25)$$

The resulting equations for the time evolution of the matrix elements of

the operators are given by (Farrell *et al.* 1988)

$$\begin{aligned}
 \langle \dot{\chi}_{e'e''} \rangle &= -i(\omega_{e''} - \omega_{e'}) \langle \chi_{e'e''} \rangle - i \sum_g \Omega_{e''g} \langle \chi_{e'g} \rangle \\
 &+ i \sum_g \Omega_{e'g} \langle \chi_{ge''} \rangle \\
 &- \sum_e \sum_g \sum_\lambda g_{e''g}^\lambda g_{eg}^{\lambda*} \pi \delta(\omega_\lambda - \omega_e + \omega_g) \langle \chi_{e'e} \rangle, \\
 &- \sum_e \sum_g \sum_\lambda g_{e'g}^\lambda g_{eg}^{\lambda*} \pi \delta(\omega_\lambda - \omega_e + \omega_g) \langle \chi_{e'e''} \rangle, \tag{26a}
 \end{aligned}$$

$$\begin{aligned}
 \langle \dot{\chi}_{g'g''} \rangle &= -i(\omega_{g''} - \omega_{g'}) \langle \chi_{g'g''} \rangle - i \sum_e \Omega_{eg''} \langle \chi_{g'e} \rangle \\
 &+ i \sum_e \Omega_{eg'} \langle \chi_{eg''} \rangle \\
 &+ \sum_{e'} \sum_e \sum_\lambda g_{e'g''}^{\lambda*} g_{eg'}^\lambda \pi \delta(\omega_\lambda - \omega_e + \omega_{g'}) \langle \chi_{e'e} \rangle \\
 &+ \sum_{e'} \sum_e \sum_\lambda g_{e'g'}^{\lambda*} g_{eg''}^\lambda \pi \delta(\omega_\lambda - \omega_e + \omega_{g''}) \langle \chi_{e'e} \rangle, \tag{26b}
 \end{aligned}$$

$$\begin{aligned}
 \langle \dot{\chi}_{e'g'} \rangle &= -i\Delta_{e'g'} \langle \chi_{e'g'} \rangle + i \sum_g \Omega_{e'g} \langle \chi_{gg'} \rangle \\
 &- i \sum_e \Omega_{eg'} \langle \chi_{e'e} \rangle \\
 &- \sum_e \sum_g \sum_\lambda g_{e'g}^{\lambda*} g_{eg}^\lambda \pi \delta(\omega_\lambda - \omega_e + \omega_g) \langle \chi_{eg'} \rangle. \tag{26c}
 \end{aligned}$$

Here, it has been assumed that $|g\rangle$ is a ground state of the atom. A more general set of equations has been given in MacGillivray and Standage (1988) for the case where the lower state is not a ground state.

The triple summation terms in these equations represent the relaxation processes, with the generalised decay term being given by

$$\begin{aligned}
 \Gamma_{e'e''g} &= \sum_\lambda [g_{e'g}^{\lambda*} g_{e''g}^\lambda \pi \delta(\omega_\lambda - \omega_{e''} + \omega_g) \\
 &+ g_{e''g}^\lambda g_{e'g}^{\lambda*} \pi \delta(\omega_\lambda - \omega_{e'} + \omega_g)]. \tag{27}
 \end{aligned}$$

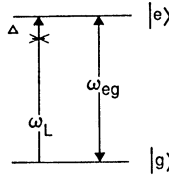
The decay rate from state $|e'\rangle$ to $|g\rangle$ is given by

$$\Gamma_{e'g} = \Gamma_{e'e'g}, \tag{28}$$

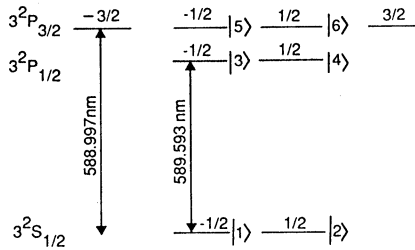
while the total decay rate from the excited state $|e'\rangle$ is

$$\Gamma_{e'} = 2 \sum_g \sum_\lambda |g_{e'g}^\lambda|^2 \pi \delta(\omega_\lambda - \omega_{e'} + \omega_g). \tag{29}$$

(a)



(b)



(c)

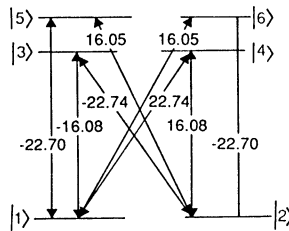


Fig. 2. (a) Two-level excitation scheme. (b) J representation of the Na-D transitions. (c) Six-level excitation scheme for the Na-D transitions under π excitation. Rabi frequencies per unit square-root intensity [MHz/(mW/mm²)^{1/2}] are shown. The overall decay constant is $6.25 \times 10^7 \text{ s}^{-1}$.

To illustrate the differences between the semiclassical and Heisenberg operator techniques with a realistic example, a three-state system is considered (Fig. 2) in which each state consists of two degenerate substates. This system is the J -representation energy level scheme for the Na-D transitions. All excited states are connected to the ground state by optical transitions and π polarisation has been assumed for the single mode, laser excitation. The Rabi frequencies for the transitions are also shown in Fig. 2c. Whereas the excitation of both the $3^3P_{3/2}$ and $3^2P_{1/2}$ levels of sodium with a single mode laser is unlikely, this configuration serves to illustrate the application of the QED

approach without resorting to the more complicated hyperfine representation. Application of equations (26) to this case results in the following equations:

$$\begin{aligned}
 \langle \dot{\chi}_{66} \rangle &= -i\Omega_{62}(\langle \chi_{62} \rangle - \langle \chi_{26} \rangle) - \Gamma_6 \langle \chi_{66} \rangle, \\
 \langle \dot{\chi}_{55} \rangle &= -i\Omega_{51}(\langle \chi_{51} \rangle - \langle \chi_{15} \rangle) - \Gamma_5 \langle \chi_{55} \rangle, \\
 \langle \dot{\chi}_{44} \rangle &= -i\Omega_{42}(\langle \chi_{42} \rangle - \langle \chi_{24} \rangle) - \Gamma_4 \langle \chi_{44} \rangle, \\
 \langle \dot{\chi}_{33} \rangle &= -i\Omega_{31}(\langle \chi_{31} \rangle - \langle \chi_{13} \rangle) - \Gamma_3 \langle \chi_{33} \rangle, \\
 \langle \dot{\chi}_{22} \rangle &= -i\Omega_{42}(\langle \chi_{24} \rangle - \langle \chi_{42} \rangle) - i\Omega_{62}(\langle \chi_{26} \rangle - \langle \chi_{62} \rangle) \\
 &\quad + \Gamma_{32} \langle \chi_{33} \rangle + \Gamma_{42} \langle \chi_{44} \rangle + \Gamma_{52} \langle \chi_{55} \rangle + \Gamma_{62} \langle \chi_{66} \rangle \\
 &\quad + \Gamma_{532}(\langle \chi_{35} \rangle + \langle \chi_{53} \rangle) + \Gamma_{642} \langle \chi_{46} \rangle + \langle \chi_{64} \rangle, \\
 \langle \dot{\chi}_{11} \rangle &= -i\Omega_{31}(\langle \chi_{13} \rangle - \langle \chi_{31} \rangle) - i\Omega_{51}(\langle \chi_{15} \rangle - \langle \chi_{51} \rangle) \\
 &\quad + \Gamma_{31} \langle \chi_{33} \rangle + \Gamma_{41} \langle \chi_{44} \rangle + \Gamma_{51} \langle \chi_{55} \rangle + \Gamma_{61} \langle \chi_{66} \rangle \\
 &\quad + \Gamma_{531}(\langle \chi_{35} \rangle + \langle \chi_{53} \rangle) + \Gamma_{641}(\langle \chi_{46} \rangle + \langle \chi_{64} \rangle), \tag{30} \\
 \langle \dot{\chi}_{62} \rangle &= -(i\Delta + \Gamma_6/2) \langle \chi_{62} \rangle - i\Omega_{42} \langle \chi_{64} \rangle - i\Omega_{62}(\langle \chi_{66} \rangle - \langle \chi_{22} \rangle), \\
 \langle \dot{\chi}_{51} \rangle &= -(i\Delta + \Gamma_5/2) \langle \chi_{51} \rangle - i\Omega_{31} \langle \chi_{53} \rangle - i\Omega_{51}(\langle \chi_{55} \rangle - \langle \chi_{11} \rangle), \\
 \langle \dot{\chi}_{42} \rangle &= -(i\Delta' + \Gamma_4/2) \langle \chi_{42} \rangle - i\Omega_{62} \langle \chi_{46} \rangle - i\Omega_{42}(\langle \chi_{44} \rangle - \langle \chi_{22} \rangle), \\
 \langle \dot{\chi}_{31} \rangle &= -(i\Delta' + \Gamma_3/2) \langle \chi_{31} \rangle - i\Omega_{51} \langle \chi_{35} \rangle - i\Omega_{31}(\langle \chi_{33} \rangle - \langle \chi_{11} \rangle), \\
 \langle \dot{\chi}_{64} \rangle &= -i[\Delta'' + (\Gamma_4 + \Gamma_6)/2] \langle \chi_{64} \rangle - i\Omega_{42} \langle \chi_{62} \rangle + i\Omega_{62} \langle \chi_{24} \rangle, \\
 \langle \dot{\chi}_{53} \rangle &= -i[\Delta'' + (\Gamma_3 + \Gamma_5)/2] \langle \chi_{53} \rangle - i\Omega_{31} \langle \chi_{51} \rangle + i\Omega_{51} \langle \chi_{13} \rangle. \tag{31}
 \end{aligned}$$

Not shown are the six complex conjugate equations for the off-diagonal matrix elements. This set of eighteen equations forms a closed subset of the total system of thirty-six equations. The only elements contained in this set are those representing the populations, optical coherences and coherences formed by the excitation between excited state substates of different J but same m_J . These latter coherences are called vertical coherences. It was the discovery of these closed subsets of equations that made the computation of the time evolution of even more complicated atomic configurations feasible.

An interesting feature of the diagonal density matrix equations is that only the equations for the ground states contain generalised relaxation terms. This is because all the generalised relaxation terms in the equations for the excited states are grouped in pairs of terms, such as $\Gamma_{641} + \Gamma_{642}$, which cancel. Other relaxation terms of the type Γ_{eg} , which represent spontaneous decay rates between pairs of excited and ground states, also only appear in these equations. The spontaneous emission processes associated with the state populations proceed at the natural relaxation rate for each level, whereas

the optical coherences decay at half this rate. The oscillatory terms of the form $i\Delta$ for the optical coherences arise from the detuning of the laser from the atomic transition, whereas the corresponding terms for the vertical state coherences represent the fine state splitting and give rise to quantum beats. The Rabi frequency terms describe the stimulated emission and absorption processes caused by the optical interaction of the laser light with the atom.

The difference between the Heisenberg operator equations and the equations which would be obtained using the semiclassical density operator theory is the presence of the generalised relaxation terms. As mentioned above, the semiclassical theory requires the insertion of all spontaneous emission terms in an ad hoc manner, whereas these terms, as well as the generalised relaxation terms appear naturally in the full QED method. This is obviously an important consideration in the treatment of complex transitions. Further details, together with a comparison of calculations for the Na-D₂ transition using the Heisenberg operator theory and various semiclassical approximations used by other workers, can be found in Farrell *et al.* (1988). In their paper, methods are discussed for considerably reducing the magnitude of the computational task involved in performing such calculations.

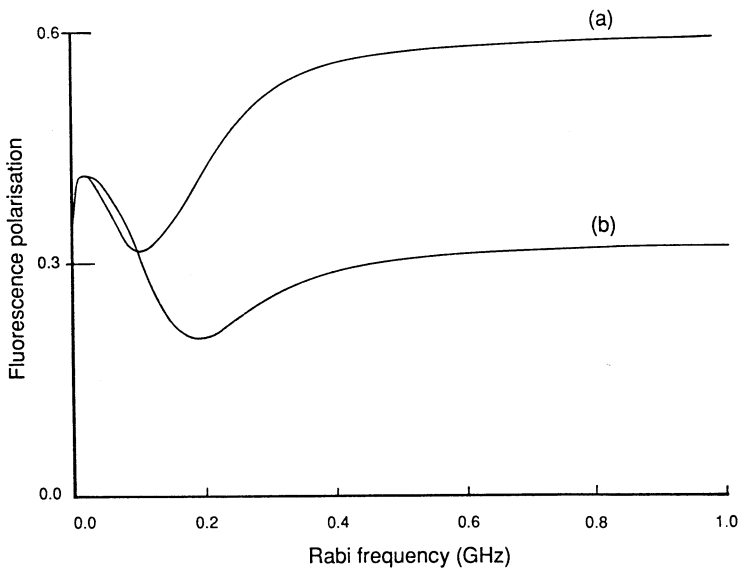


Fig. 3. Fluorescence line polarisation for the Na-D $3^2P_{3/2}(F=3, 2, 1)-3^2S_{1/2}(F'=2)$ hyperfine transition as a function of Rabi frequency. Incident single-mode laser radiation is assumed to be linearly polarised perpendicular to the fluorescence observation direction. Curve (a), full Heisenberg operator calculation; curve (b), vertical coherences and generalised relaxation terms set to zero.

Two applications of the Heisenberg operator theory are now considered. The first of these is the calculation of the line polarisation of the Na $3^2P_{3/2}(F=3, 2, 1)-3^2S_{1/2}(F'=2)$ transition as a function of laser intensity. Fig. 3 shows the results of this calculation in which it is assumed that the Doppler width of the atoms is essentially zero and the atoms are excited in a laser

beam of uniform intensity. Other calculations in which such experimental factors as the Doppler width, the laser beam intensity profile and the laser detuning are included are presented in MacGillivray and Standage (1990) and Meng *et al.* (1990). Two curves are shown in the figure; curve (a) is the result of a calculation in which the full Heisenberg operator theory has been used. Curve (b) is the result obtained when the vertical coherences and their associated generalised relaxation terms have been removed. Although the curves are similar at lower Rabi frequencies, as the Rabi frequency approaches the magnitude of the excited state hyperfine splittings (~ 100 MHz) of the transition, the curves differ markedly and asymptote to significantly different limits at high intensity. If the generalised relaxation terms are removed, but the vertical coherence terms are retained, the results obtained are very similar to the full calculation, which indicates the sensitivity of the calculation to the vertical coherences.

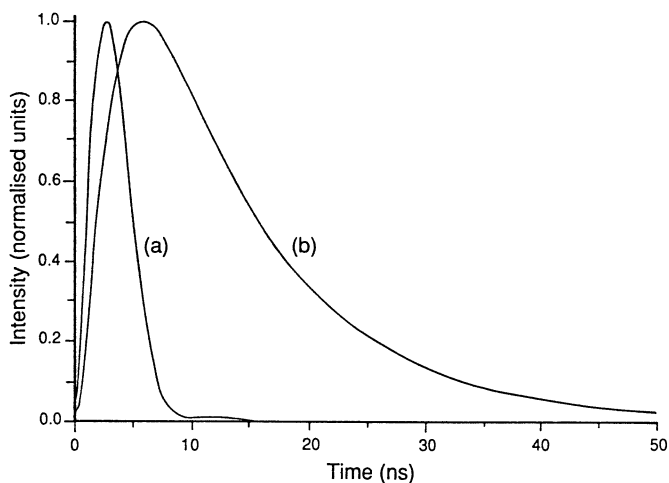


Fig. 4. Heisenberg operator calculation of stepwise coincidence signals for the $6^1S_0-6^1P_1-6^1D_2-6^3P_1$ excitation/de-excitation scheme in Hg. Curve (a), strong intensity case (130 MHz Rabi frequency); curve (b), weak intensity case (4 MHz Rabi frequency).

The second example is that of the calculation of the stepwise coincidence signal for an experiment (see Murray *et al.* 1989) with a type I scheme. The measurement of coincidences between the inelastically scattered electron and the photon emitted from the stepwise excited atom results in a time resolved coincidence signal. A calculation of the coincidence signal for the $6^1S_0-6^1P_1-6^1D_2-6^3P_1$ stepwise excitation scheme in mercury has been performed by Murray *et al.* (1990a), using the Heisenberg operator theory. Fig. 4 shows the theoretical coincidence signals obtained from this calculation. Curve (a) shows the signal predicted under strong laser excitation, in which the decay time of the signal is markedly shorter than that for the weak laser excitation case, shown in curve (b). For curve (b), the decay time is very close to the natural lifetime for the transition of 11 ns. The small secondary peak of curve (a) is the result of Rabi nutational cycling. The enhanced decay rate of the

strong excitation signal is due to the laser coupling the 11 ns lifetime upper excited state (6^1D_2) to the much shorter lived (1.3 ns), lower excited state (6^1P_1). Experimental confirmation of this effect has been found by Murray *et al.* (1990b).

4. Conclusions

In conclusion, we draw attention to the range of experimental methods now available in which lasers are applied to the investigation of collision processes. Superelastic scattering techniques have great potential for rapid data acquisition, but are presently limited in application because of the relatively limited spectral range, combined with suitable optical power, of tunable dye lasers commonly available to researchers. New developments in Ti:sapphire tunable lasers have recently extended this range into the near infra-red. It may also be possible to extend the spectral range through the development of superelastic scattering methods which are based on the use of pulsed dye lasers, that offer a greater spectral range than c.w. lasers.

The use of stepwise laser excitation combined with superelastic scattering techniques offers a means of investigating the detailed dynamics of collision processes which involve higher lying excited states and Rydberg atoms.

Stepwise electron/laser excitation offers an alternative to existing techniques for investigating collision processes that involve VUV transitions in atomic targets. In addition, these techniques provide a means of studying collision processes that involve the excitation of metastable states. It can be anticipated that stepwise coincidence experiments will be performed to obtain atomic scattering parameters for metastable states. Stepwise excitation techniques also provide a method of investigating excited state-excited state transitions. Another aspect of stepwise excitation methods is that quite a few atoms have type I excitation schemes that lie within the spectral range of dye lasers, so that the technique has fairly wide applicability.

Laser-assisted collision processes which involve inelastic electron scattering are an interesting area of recent research activity and it can be anticipated that more investigations will be carried out to compare theoretical predictions with experiment, perhaps using hydrogen rather than helium, as the atomic target.

Laser cooling techniques have not as yet been applied in collision experiments, but such techniques have been used to reduce the Doppler width of atomic beams and it is possible that laser cooling could be combined with the experimental methods discussed in this paper. The development of laser light traps to capture single atoms is presently the basis of intensive research interest. It is interesting to speculate on the application of such techniques to scattering experiments.

Considerable progress has been made in recent years in the theoretical treatment of atom-laser interactions, with methods now available which range from weak perturbative treatments, through to full quantum electrodynamical calculations that closely model complicated atomic transitions over a wide range of experimental conditions. Even the most sophisticated of these calculations is now within the capacity of computing facilities that are now widely available and we would urge colleagues to consider using such 'complete' treatments.

References

- Ackerhalt, J.R., and Eberly, J.H. (1974). *Phys. Rev. D* **10**, 3350.
- Ackerhalt, J.R., Knight, P.L., and Eberly, J.H. (1973). *Phys. Rev. Lett.* **30**, 456.
- Blum, K. (1981). 'Density Matrix Theory and Applications' (Plenum: New York).
- Dobryshin, V.E., Rakhovskii, V.I., and Shustryakov, V.M. (1982). *Opt. Spectrosc.* **52**, 609.
- Eminyan, M., MacAdam, K.B., Slevin, J., and Kleinpoppen, H. (1974). *J. Phys. B* **7**, 1519.
- Farrell, P.M., MacGillivray, W.R., and Standage, M.C. (1988). *Phys. Rev. A* **37**, 4240.
- Farrell, P.M., Webb, C.J., MacGillivray, W.R., and Standage, M.C. (1989). *J. Phys. B* **22**, L527.
- Francken, P., and Attaourti, Y. (1988). *Phys. Rev. A* **38**, 1785.
- Gallagher, A. (1987). personal communication.
- Hanne, G.F., Szmytkowski, Cz., and Van Der Wiel, M. (1982). *J. Phys. B* **15**, L109.
- Hanne, G.F., Nickich, V., and Sohn, M. (1985). *J. Phys. B* **18**, 2037.
- Hermann, H.W., Hertel, I.V., Reiland, W., Stamatovic, A., and Stoll, W. (1977). *J. Phys. B* **10**, 251.
- Hermann, H.W., Hertel, I.V., and Kelley, M.H. (1980). *J. Phys. B* **13**, 3465.
- Hertel, I.V., and Stoll, W. (1974). *J. Phys. B* **7**, 570.
- Hertel, I.V., and Stoll, W. (1977). *Adv. At. Mol. Phys.* **13**, 113.
- Jaduszliwer, B., Weiss, P., Tino, A., and Bederson, B. (1984). *Phys. Rev. A* **30**, 1255.
- MacGillivray, W.R., and Standage, M.C. (1988). *Phys. Rep.* **168**, 1.
- MacGillivray, W.R., and Standage, M.C. (1990). *Comments At. Mol. Phys.* (in press).
- McClelland, J.J., Kelley, M.H., and Celotta, R.J. (1989). *Phys. Rev. A* **40**, 2321.
- McLucas, C.W., MacGillivray, W.R., and Standage, M.C. (1982a). *Phys. Rev. Lett.* **48**, 88.
- McLucas, C.W., Wehr, H.J.W., MacGillivray, W.R., and Standage, M.C. (1982b). *J. Phys. B* **15**, 1883.
- Mason, N.J., and Newell, W.R. (1987). *J. Phys. B* **20**, L 323.
- Mason, N.J., and Newell, W.R. (1989). *J. Phys. B* **22**, 777.
- Meng, X.-K., MacGillivray, W.R., and Standage, M.C. (1990). in preparation.
- Miers, R.E., Gastineau, J.E., Phillips, M.H., Anderson, L.W., and Lin, C.C. (1982). *Phys. Rev. A* **25**, 1185.
- Murray, A.J., Webb, C.J., MacGillivray, W.R., and Standage, M.C. (1989). *Phys. Rev. Lett.* **62**, 411.
- Murray, A.J., MacGillivray, W.R., and Standage, M.C. (1990a). *J. Phys. B* (in press).
- Murray, A.J., MacGillivray, W.R., and Standage, M.C. (1990b). In preparation.
- Phelps, J.O., Phillips, M.H., Anderson, L.W., and Lin, C.C. (1982). *Phys. Rev. A* **25**, 1185.
- Phillips, M.H., Anderson, L.W., and Lin, C.C. (1981a). *Phys. Rev. A* **23**, 2751.
- Phillips, M.H., Anderson, L.W., and Lin, C.C. (1981b). *Phys. Lett. A* **82**, 404.
- Register, D.F., Trajmar, S., Jensen, S.W., and Poe, R.T. (1978). *Phys. Rev. Lett.* **41**, 749.
- Register, D.F., Trajmar, S., Csanak, G., Jensen, S.W., Fineman, M.A., and Poe, R.T. (1983). *Phys. Rev. A* **28**, 151.
- Scholten, R.E., Anderson, T., and Teubner, P.J.O. (1988). *J. Phys. B* **21**, L473.
- Stumpf, B., and Gallagher, A. (1985). *Phys. Rev. A* **32**, 3344.
- Trajmar, S., Nickel, J.C., and Zetner, P.W. (1990). 'Jet Propulsion Laboratory Report' (JPL D-7111).
- Wallbank, B., Holmes, J.K., LeBlanc, L., and Weingartshofer, A. (1988). *Z. Phys. D* **10**, 467.
- Webb, C.J., MacGillivray, W.R., and Standage, M.C. (1984a). *J. Phys. B* **17**, 1675.
- Webb, C.J., MacGillivray, W.R., and Standage, M.C. (1984b). *J. Phys. B* **17**, 2377.
- Webb, C.J., MacGillivray, W.R., and Standage, M.C. (1985a). *J. Phys. B* **18**, 1701.
- Webb, C.J., MacGillivray, W.R., and Standage, M.C. (1985b). *J. Phys. B* **18**, L259.
- Weingartshofer, A., Holmes, J.K., Caudle, G., Clarke, E.M., and Kruger, H. (1977). *Phys. Rev. Lett.* **39**, 269.
- Whitley, R.M., and Stroud, C.R. (1976). *Phys. Rev. A* **14**, 1498.
- Zetner, P.W., Westerweld, W.B., King, G.C., and McConkey, J.W. (1986). *J. Phys. B* **16**, 4205.
- Zetner, P.W., Trajmar, S., Csanak, G., and Clark, R.E.H. (1989). *Phys. Rev. A* **39**, 6022.

